



A physically based methodology for predicting anisotropic creep properties of Ni-based superalloys

Jia Huang, Duo-Qi Shi* , Xiao-Guang Yang

Received: 13 May 2014/Revised: 1 July 2014/Accepted: 8 June 2015/Published online: 5 July 2015
© The Nonferrous Metals Society of China and Springer-Verlag Berlin Heidelberg 2015

Abstract This paper is focused on developing suitable methodology for predicting creep characteristics (i.e., the minimum creep strain rate, stress rupture life and time to a specified creep strain) of typical Ni-based directionally solidified (DS) and single-crystal (SC) superalloys. A modern method with high accuracy on simulating wide ranging creep properties was fully validated by a sufficient amount of experimental data, which was then developed to model anisotropic creep characteristics by introducing a simple orientation factor defined by the ultimate tensile strength (UTS). Physical confidence on this methodology is provided by the well-predicted transitions of creep deformation mechanisms. Meanwhile, this method was further adopted to innovatively evaluate the creep properties of different materials from a relative perspective.

Keywords Wilshire equations; Anisotropic creep properties; Ni-based superalloy; Prediction methodology; Creep mechanism

1 Introduction

Nowadays, the Ni-based superalloys have been widely used in the manufacture of gas turbine engine components that are subjected to highly aggressive environment (such as high inlet gas temperatures, high centrifugal loads) in the process of long-term service, and then the creep deformation and stress rupture behavior of these components are important safe limiting factors [1]. For the safety

and economic reasons, considerable efforts were exerted to gain a fundamental understanding of creep mechanisms [2]. However, for the high test cost and time-consuming creep test, it is not practicable to carry out extensive experimental investigations to account for all the possible stress–temperature states. Hence, with lower cost and shorter period, it is significant to develop accurate predictions models for simulating creep characteristics. Currently, the traditional methodologies involving power law equations are not sufficient to describe creep behavior in a wide range of stress–temperature conditions [3], which leads to an appearance of more modern techniques such as the Theta projection method [4], the hyperbolic tangent [5] and the Wilshire equations [3]. Up to now, the Wilshire equations developed at Swansea University by Wilshire and Scharning [6] have been validated on predicting typical creep behaviors (i.e., the minimum creep strain rate ($\dot{\epsilon}_{\min}$), stress rupture life (t_f) and time to a specified creep strain (t_c)) with good extrapolation performance, reasonable temperature capability and availability. The applications were successfully carried out in steel, copper, aluminum alloy and Ni-based polycrystalline superalloy in a wide range of stress–temperature conditions [3, 7]; especially, the modified creep activation energy is close to the lattice self-diffusion energy and breaks seen in the equations are consistent with the observed creep deformation mechanism, which turns to be the physical confidence of this technique. However, validation of this new methodology requires more evidence on its applicability to a wide range of materials, particularly the advanced Ni-based superalloys widely used in the aerospace industry. Meanwhile, compared with the conventional polycrystalline Ni-based superalloys, the directionally solidified (DS) (or single-crystal (SC)) superalloys were developed by eliminating

J. Huang, D.-Q. Shi*, X.-G. Yang
School of Energy and Power Engineering, Beihang University,
Beijing 100191, China
e-mail: shdq@buaa.edu.cn

transverse (or any) grain boundaries to provide superior mechanical properties and good corrosion resistance at elevated temperatures. However, the lack of grain boundaries also leads to highly anisotropic material mechanical properties [8], especially in low-cycle fatigue (LCF) and creep behavior [9, 10]. Up to now, the anisotropic creep properties have been investigated adequately by experiments, but little attention was paid to the unified simulation methods for predicting the anisotropic creep behaviors.

In this paper, the capability of Wilshire equations on simulating creep characteristics of typical Ni-based superalloys was verified comprehensively, and then a simple orientation factor defined by ultimate tensile strength (UTS) was introduced to consider the influence of crystal orientation. The physical confidence on this method was also discussed, and the innovative application on Wilshire curves was further carried out with the perspective on full utilization of creep property.

2 Experimental data and analysis

2.1 Experimental data

In this paper, a sufficient amount of experimental creep characteristics data (i.e., $\dot{\epsilon}_{\min}$, t_f and t_e) were collected for full verifying the feasibility of Wilshire equations, where a wide range of typical Ni-based DS and SC superalloys commonly used in gas turbine applications was adopted (i.e., DS superalloys DZ125 [11, 12], DZ17G [10, 11, 13], DS GTD-111 [14–16] and SC superalloys: CMSX-4 [17–19]). The data at different crystal orientations were also contained for verifying capability of the improved Wilshire method. The detailed data are shown later by the comparison with the master predicted curves. The corresponding experimental procedures can be found from the above-cited literatures. It should be noted that all the mentioned units in this paper are as follows: temperature (T) in K, creep strain rate ($\dot{\epsilon}$) in h^{-1} and time (t) in h.

2.2 Analysis by traditional power law expression

Since the early 1950s, the most commonly used power law equation for correlating t_f with $\dot{\epsilon}_{\min}$ at high temperatures shown in Eq. (1) was proposed by Monkman and Grant [20]. $\dot{\epsilon}_{\min}$ described by Dorn equation [21] is shown in Eq. (2):

$$M = t_f \dot{\epsilon}_{\min} \quad (1)$$

$$\dot{\epsilon}_{\min} = A\sigma^n \exp(-Q_c/RT) \quad (2)$$

where M is material constant and $R = 8.314 \text{ J}\cdot\text{K}^{-1}\cdot\text{mol}^{-1}$, T is Kelvin temperature, A and stress exponent n are

material parameters dependent on stress and temperature and Q_c is the creep activation energy fitted at constant applied stress (σ). In this section, the above-mentioned power law expression was adopted to predict the stress rupture property of a typical Ni-based DS superalloy DZ125 and the parameter stability was discussed. As shown in Fig. 1a, the stress rupture tests of DZ125 were carried out under a wide range of stress–temperature conditions and the obtained rupture data show obvious temperature and stress dependence. Although the longitudinal (L) direction exhibits overall longer life for each temperature, the anisotropic behavior is pronounced at the lower temperature of 760 °C and is evidently reduced at the higher temperature. The influence of orientation on the stress rupture properties will be uniformly predicted later. It should be noted that, in this paper, the basic assumption is made that the creep rupture behavior is strain controlled and the rupture life is closely connected with $\dot{\epsilon}_{\min}$ [22]. According to Eqs. (1) and (2), the stress exponents of DZ125 at L direction under different temperatures can be linearly fitted by plotting $\ln t_f$ versus $\ln \sigma$. The values calculated by slopes are 14.00 for 760 °C, 5.90 for 850 °C, 5.36 for 900 °C, 5.48 for 980 °C, 4.79 for 1040 °C and 4.60 for 1093 °C, respectively. A roughly decrease in the values of n occurs with the increase in temperature. Meanwhile, the creep activation energy (Q_c) of DZ125 can also be calculated at constant applied stress (σ) under variable temperatures, which changes from 509 to 429 $\text{kJ}\cdot\text{mol}^{-1}$. That is to say, the parameters n and Q_c in Eq. (2) seem to be stress and temperature dependent, which is consistent with the researches on other materials [22]. Hence, the prediction accuracy of the traditional power law expression is accepted only within a limited range of stress and temperature conditions. These intangible variations of the parameters with the change of test conditions make accurate extrapolation of creep properties impossible.

Subsequently, many studies revealed that the stress dependence on $\dot{\epsilon}_{\min}$ at different temperatures can be eliminated by normalizing σ through the yield stress (σ_{yield} or UTS (σ_{TS})) [3]. However, σ_{TS} is usually chosen because it can be carried out with stresses ranging from $\sigma/\sigma_{\text{TS}} = 1$ to $\sigma/\sigma_{\text{TS}} = 0$. Hence, Eq. (1) evolves into Eq. (3):

$$M/t_f = \dot{\epsilon}_{\min} = A^*(\sigma/\sigma_{\text{TS}})^n \exp(-Q_c^*/RT) \quad (3)$$

where $A^* \neq A$ and Q_c^* are determined by plotting ($\ln \dot{\epsilon}_{\min}$) or ($\ln t_f$) against ($1/T$) at constant $\sigma/\sigma_{\text{TS}}$. The value of Q_c^* for DZ125 is 302.04 $\text{kJ}\cdot\text{mol}^{-1}$. Hence, by plotting $\ln(\sigma/\sigma_{\text{TS}})$ against $\ln[t_f \exp(-Q_c^*/(RT))]$, it can be seen that the stress rupture data of DZ125 (Fig. 1a) at different temperatures are superimposed onto a single curve (Fig. 1b). However, the stress exponent (n) in Eq. (3) is still varied (i.e., ranges

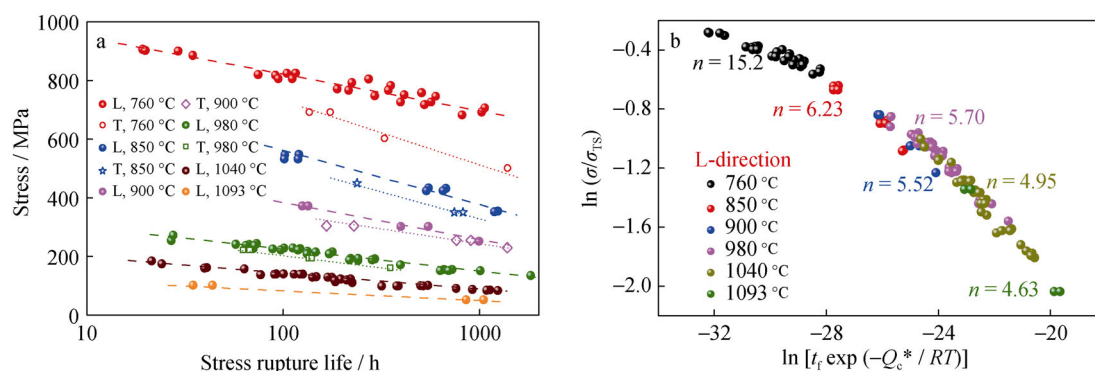


Fig. 1 Stress rupture property **a** and application of UTS-normalized power law equations **b** of DZ125

from 15.20 to 4.63) with the change of stress level, and once again, this instability of n makes prediction and extrapolation impossible.

3 Estimation of original Wilshire equations

3.1 Original Wilshire equations

According to the above-mentioned application of the traditional power law equations on DZ125, it can be found that the variability in values of n and Q_c makes predicting creep properties over a wide range of test conditions difficult. Meanwhile, it should be noted that, for any material, applying a stress equals to σ_{TS} at any given temperature will result in near instantaneous rupture, and creep rupture cannot be expected if the applied stress equals to zero [3]. That is to say, $t_f \rightarrow 0$ and $\dot{\epsilon}_{min} \rightarrow \infty$ occur when $\sigma/\sigma_{TS} \rightarrow 1$, and then $t_f \rightarrow \infty$ and $\dot{\epsilon}_{min} \rightarrow 0$ occur as $\sigma/\sigma_{TS} \rightarrow 0$. There is no doubt that the stress ranging from 0 to σ_{TS} must be considered in a robust method for predicting creep properties in a wide range of stress conditions. However, when Eq. (3) was rewritten into Eq. (4), it can be seen that this type of power law expression does not meet the basic physical response which occurs with stresses ranging from 0 to σ_{TS} .

$$\sigma/\sigma_{TS} = \left\{ M/A^* \times [t_f \exp(-Q_c^*/RT)]^{-1} \right\}^{\frac{1}{n}} \quad (4)$$

Fortunately, in order to effectively avoid these unpredictable n value variations, the more recently developed Wilshire equations, devised at Swansea University by Wilshire et al. [7], follow the analogous sigmoidal descriptions of creep properties (i.e., $\dot{\epsilon}_{min}$, t_f and t_e) to consider the above-mentioned stress variation from 0 to σ_{TS} . The corresponding equations evolved from the traditional power law equations are shown in Eqs. (5)–(7).

$$\frac{\sigma}{\sigma_{TS}} = \exp \left\{ -k_1 \left[t_f \exp \left(\frac{-Q_c^*}{RT} \right) \right]^u \right\} \quad (5)$$

$$\frac{\sigma}{\sigma_{TS}} = \exp \left\{ -k_2 \left[\dot{\epsilon}_{min} \exp \left(\frac{Q_c^*}{RT} \right) \right]^v \right\} \quad (6)$$

$$\frac{\sigma}{\sigma_{TS}} = \exp \left\{ -k_3 \left[t_e \exp \left(\frac{-Q_c^*}{RT} \right) \right]^w \right\} \quad (7)$$

where the parameters Q_c^* , k_1 , k_2 , k_3 , u , v and w are derivable from a reasonably comprehensive set of creep rupture data. Although the capability of the Wilshire equations was proved in many materials, few applications were carried out on the advanced Ni-based superalloys. Hence, the validity of Wilshire equations was carefully proved on DZ125 as follows.

3.2 Prediction results

To illustrate the capability of this model, the activation energy (Q_c^*) should be firstly estimated by plotting $\ln \dot{\epsilon}_{min}$ or $\ln t_f$ against $1/T$ at constant σ/σ_{TS} , which ensures that Q_c^* remains constant regardless of testing temperature. Concretely, the values of Q_c^* are 302.04, 307.93 and 262.1 kJ·mol⁻¹ for DZ125, DS GTD-111 and CMSX-4, respectively. Then, the remaining constants in each equation can be further determined by linear fitting. For example, by plotting $\ln[t_f \exp(-Q_c^*/RT)]$ against $\ln[-\ln(\sigma/\sigma_{TS})]$, the constants u and k_1 can be calculated by the gradient and intercept. Finally, the predicted creep properties at different test conditions are compared with the experimental data published in cited literatures. The validation of Wilshire equations was carried out on $\dot{\epsilon}_{min}$, t_f and t_e , respectively.

3.2.1 Stress rupture life (t_f)

By plotting $\ln[t_f \exp(-Q_c^*/RT)]$ against $\ln[-\ln(\sigma/\sigma_{TS})]$, the predicted stress rupture lives under different testing conditions of DZ125 are shown in Fig. 2a, from which it can

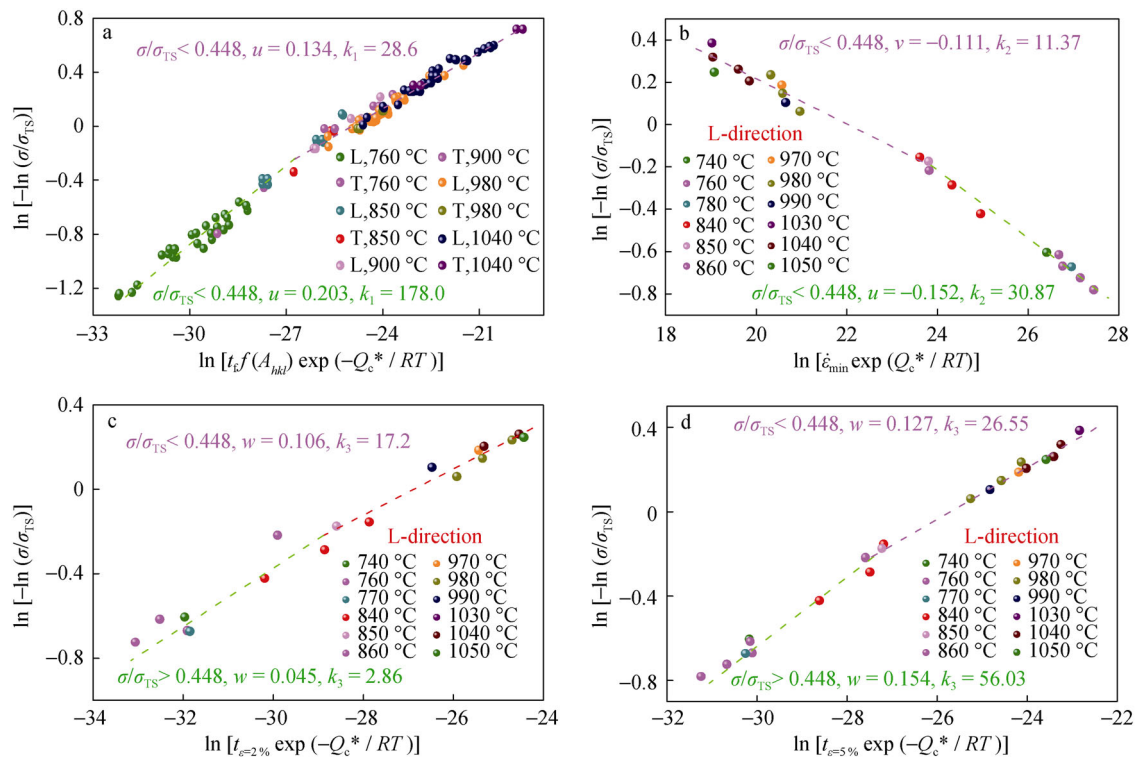


Fig. 2 Creep properties of DZ125 predicted by Wilshire method: **a** stress rupture life, **b** minimum creep strain rate, **c** time to creep strain ($\epsilon = 2\%$) and **d** time to creep strain ($\epsilon = 5\%$)

seen that t_r (obtained in a wide range of testing conditions) of DZ125 can be well described by Wilshire equations. The predicted master curves are interrupted into two continuous lines, and the physical basic for the predicted break points by this method will be discussed in detail later. For DZ125, the values of u and k_1 are 0.134 and 28.6 for $\sigma/\sigma_{TS} < 0.448$, while 0.203 and 178.0 for $\sigma/\sigma_{TS} > 0.448$. The predicted stress rupture lives at transverse (T) direction by the improved method are also exhibited in Fig. 2 but will be discussed later.

3.2.2 Minimum creep strain rate ($\dot{\epsilon}_{min}$)

Once again, the constants v and k_2 in Eq. (6) can also be calculated easily by the gradient and intercept in the plot of $\ln[\dot{\epsilon}_{min} \exp(Q_c^*/RT)]$ against $\ln[-\ln(\sigma/\sigma_{TS})]$. As shown in Fig. 2b, it can be concluded that $\dot{\epsilon}_{min}$ of DZ125 can be well predicted. Compared with Fig. 2a, it is encouraging that the break point locates at the same level of σ/σ_{TS} . The values of v and k_2 are -0.111 and 11.37 for $\sigma/\sigma_{TS} < 0.448$, whereas they are -0.152 and 30.87 for $\sigma/\sigma_{TS} > 0.448$.

3.2.3 Time to a specified strain (t_ϵ)

To predict the time to a specified creep strain, similar prediction was carried out by plotting $\ln[t_\epsilon \exp(-Q_c^*/RT)]$

against $\ln[-\ln(\sigma/\sigma_{TS})]$. As shown in Fig. 2c, d, the needed t_ϵ to reach two specified creep strains of DZ125 is well described, where similar locations of break points also exist as before. When the specimens are crept to 2% strain, the values of w and k_3 are 0.106 and 17.2 for $\sigma/\sigma_{TS} < 0.448$, while 0.125 and 29.5 for $\sigma/\sigma_{TS} > 0.448$. When the specimens are even crept to a bigger strain of 5%, the needed time can also be well predicted and the values of w and k_3 are 0.127 and 26.55 for $\sigma/\sigma_{TS} < 0.448$, while 0.154 and 56.03 for $\sigma/\sigma_{TS} > 0.448$.

4 Improved Wilshire equations

It was proved that the creep properties along a specified crystal direction of DZ125 (i.e., L direction) can be well simulated by the original Wilshire equations. However, the creep properties of DS and SC superalloys are inherently anisotropic [23]. Up to now, the Wilshire equations have not been further conducted for predicting anisotropic creep characteristics uniformly, which turns to be the other purpose of this article. To consider the influence of orientation on $\dot{\epsilon}_{min}$, Guo et al. reported that the anisotropic $\dot{\epsilon}_{min}$ was due to the elastic anisotropy, and then Eq. (2) turns to be Eq. (8) as follows [13]:

$$\dot{\epsilon}_{min} = B(\sigma/E)^n \exp(-Q_c/RT) \tag{8}$$

where B is the material parameter, E is the Young's modulus and Q_c is assumed to be orientation independent. They found that the anisotropic behavior of $\dot{\epsilon}_{\min}$ can be well described by this simply modified equations. Although this equation was validated in a limited stress–temperature condition, it is encouraged to assume that the anisotropic creep properties are consistent with orientation-related material property parameter. According to the orientation dependence on t_f of DZ125 with the increase in temperature as shown in Fig. 1a, it can be concluded that in a wide range of stress-temperature conditions, the anisotropic t_f exhibits better consistency with UTS (Fig. 3a) rather than Young's modulus (Fig. 3b). Hence, it is assumed that the influence of crystal orientation on creep properties can be simply considered by the compensation function of UTS. Concretely, $\dot{\epsilon}_{\min}$ in any crystal orientation $[hkl]$ is supposed to be described by the introduction of an orientation factor, $f(A_{hkl}) = \sigma_{TS,[001]} / \sigma_{TS,[hkl]}$, then Eq. (8) now becomes:

$$f(A_{hkl}) = \sigma_{TS,[001]} / \sigma_{TS,[hkl]} \tag{9}$$

$$\dot{\epsilon}_{\min} = C(f(A_{hkl})\sigma)^n \exp(-Q_c/(RT)) \tag{10}$$

where A_{hkl} is the orientation factor, $\sigma_{TS,[001]}$ is UTS at $[001]$ orientation, $\sigma_{TS,[hkl]}$ is UTS at one crystal orientation $[hkl]$ and C is material parameter. By plotting $\ln \dot{\epsilon}_{\min}$ against $\ln[f(A_{hkl})\sigma]$ as shown in Fig. 4, it can be concluded that, to a certain extent, the anisotropic $\dot{\epsilon}_{\min}$ of DZ17G and DS GTD-111 at different temperatures can be well described by Eqs. (9) and (10). Subsequently, following the same evolution from Eq. (1) with help of Eq. (2) to the original Wilshire equations, the orientation factor modified Wilshire equations are now shown as follows:

$$\frac{\sigma}{\sigma_{TS}} = \exp\left\{-k_1 \left[f(A_{hkl})t_f \exp\left(\frac{-Q_c^*}{RT}\right) \right]^u\right\} \tag{11}$$

$$\frac{\sigma}{\sigma_{TS}} = \exp\left\{-k_2 \left[f(A_{hkl})\dot{\epsilon}_{\min} \exp\left(\frac{Q_c^*}{RT}\right) \right]^v\right\} \tag{12}$$

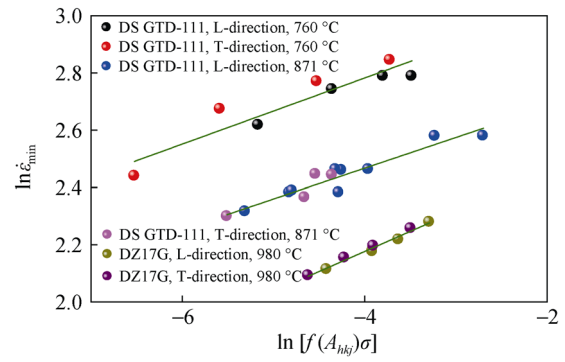


Fig. 4 Schematic expressed by $\ln \dot{\epsilon}_{\min}$ versus $\ln[f(A_{hkl})\sigma]$

$$\frac{\sigma}{\sigma_{TS}} = \exp\left\{-k_3 \left[f(A_{hkl})t_\epsilon \exp\left(\frac{-Q_c^*}{RT}\right) \right]^w\right\} \tag{13}$$

where the parameters Q_c^* are also assumed to be orientation independent, all parameters are calculated in the same way as those in Eq. (5).

Similarly, the predicted master curves of anisotropic creep properties by the improved Wilshire equations are compared with collected testing data of a Ni-based superalloy DS GTD-111. Using the same procedure as before, the simulated anisotropic creep results of DZ125 and DS GTD-111 are shown in Figs. 2a, 5 and 6, respectively. It can be seen that a very good simulation of the anisotropic creep characteristics of DS GTD-111 (i.e., $\dot{\epsilon}_{\min}$, t_f and t_ϵ ; i.e., $\epsilon = 0.3\%$, 0.5% and 1.0%) is obtained by the improved Wilshire equations. The values of the model parameters in Eq. (11) are shown in Figs. 2a, 5 and 6.

5 Discussions

5.1 Physical significance of Q_c^*

The physical significances of the model parameter Q_c^* of Wilshire equations are discussed to provide confidence to

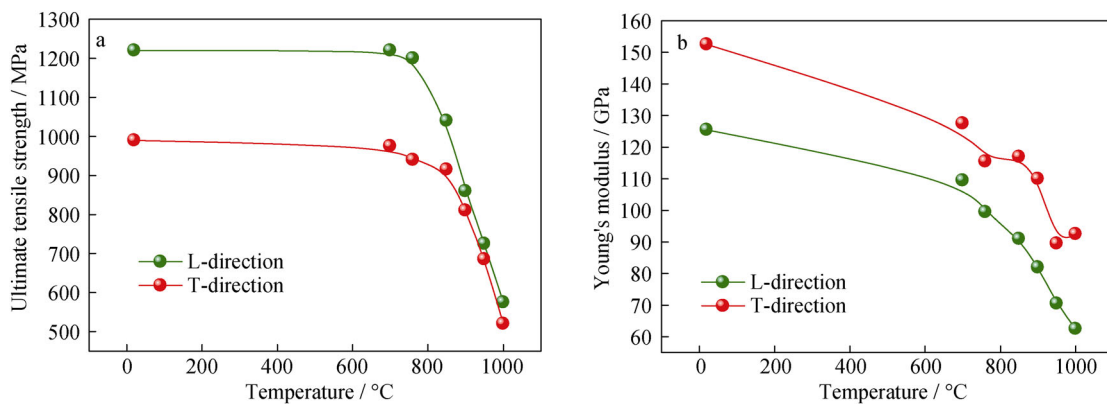


Fig. 3 Material properties of DZ125 at different temperatures: **a** UTS and **b** Young's modulus

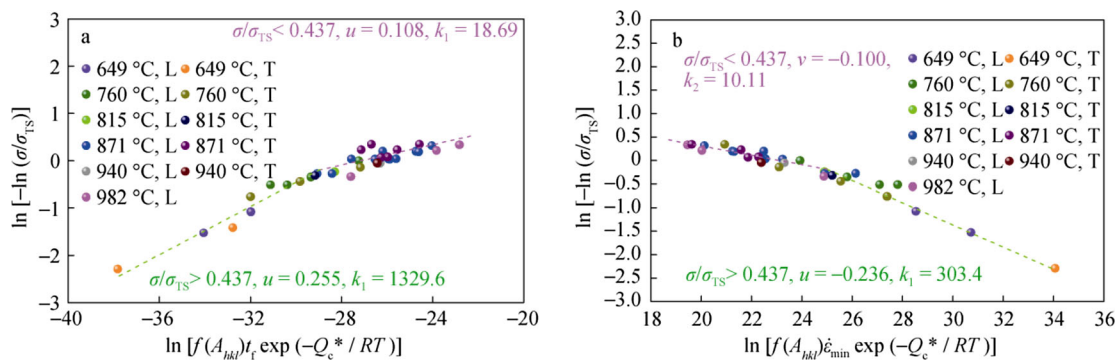


Fig. 5 Schematic expressed by **a** $\ln[f(A_{hkl})t_f \exp(-Q_c^*/RT)]$ versus $\ln[-\ln(\sigma/\sigma_{TS})]$ and **b** $\ln[f(A_{hkl})\dot{\epsilon}_{min} \exp(-Q_c^*/RT)]$ versus $\ln[-\ln(\sigma/\sigma_{TS})]$ of DS GTD-111

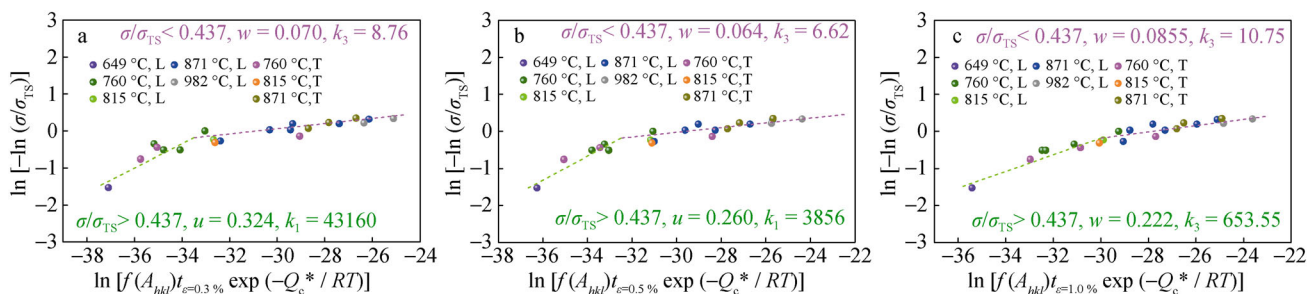


Fig. 6 Schematic expressed by $\ln[f(A_{hkl})t_{\epsilon} \exp(-Q_c^*/RT)]$ versus $\ln[-\ln(\sigma/\sigma_{TS})]$ of DS GTD-111: **a** 0.3 % strain, **b** 0.5 % strain, and **c** 1.0 % strain

this method. The values of Q_c^* are calculated from the superimposition of different temperature data sets from temperature compensated graphs of either t_f or $\dot{\epsilon}_{min}$ against normalized stress σ/σ_{TS} at each testing temperature, and previous work for a range of materials shows that this processing method provides more realistic and constant activation energy values, which compare favorably with the activation energy for lattice diffusion [24]. For the Ni-based superalloys investigated in this paper, as mentioned before, the values of Q_c^* are 302.04, 307.93 and 262.10 $\text{kJ}\cdot\text{mol}^{-1}$ for DZ125, DS GTD-111 and CMSX-4, respectively. The Q_c^* value of DZ125 is much lower than Q_c (i.e., ranging from 509 to 429 $\text{kJ}\cdot\text{mol}^{-1}$) calculated by traditional power law expressions. Meanwhile, it is reported that the self-diffusion activation energy for Ni-based superalloys is in the range of 257–283 $\text{kJ}\cdot\text{mol}^{-1}$ [25]. Hence, these obtained values are far closer to the activation energy for lattice diffusion of Ni-based superalloys than the Q_c values calculated traditionally.

5.2 Physical significance of predicted break points

It is proved that the existed ‘break point’ in the graph by plotting Wilshire equations is related to the transition of creep deformation mechanism which occurs at high and

low regions of σ/σ_{TS} , which largely helps to provide confidence to this method [3]. Currently, during the procedure of predicting t_f or $\dot{\epsilon}_{min}$ of SC superalloy CMSX-4, predicted break points are compared with the stress-level related creep mechanism published in Ref. [26]. As shown in Fig. 7a, the stress rupture data tested in a wide range of stress–temperature conditions of CMSX-4 at [001] direction were simulated, and once again, two break points clearly exist at different stress levels (i.e., $\sigma/\sigma_{TS} = 0.26$ and 0.51). Meanwhile, as shown in Fig. 7b, the creep deformation mechanism of CMSX-4 was investigated systematically before [26]. Three regimes are identified, and distinct microstructural degradation is predominant for each mode. Firstly, the specimens crept at low temperatures with high applied stress exhibit primary mode, whose characteristic is a significant heterogeneity of slip and the deformation is controlled by the movement of dislocation ribbons of net Burgers vector $a < 11\bar{2} >$. Secondly, the tertiary mode occurs in the intermediate creep regime, where the dislocation activity of the $a/2 < 1\bar{1}1 > \{111\}$ type is restricted to the γ channels between the γ' particles. The density of dislocations is found to increase with the increase in creep strain. Thirdly, the rafting mode happens at high temperature with low applied stress, where the γ/γ' microstructure degrades rather quickly for thermally

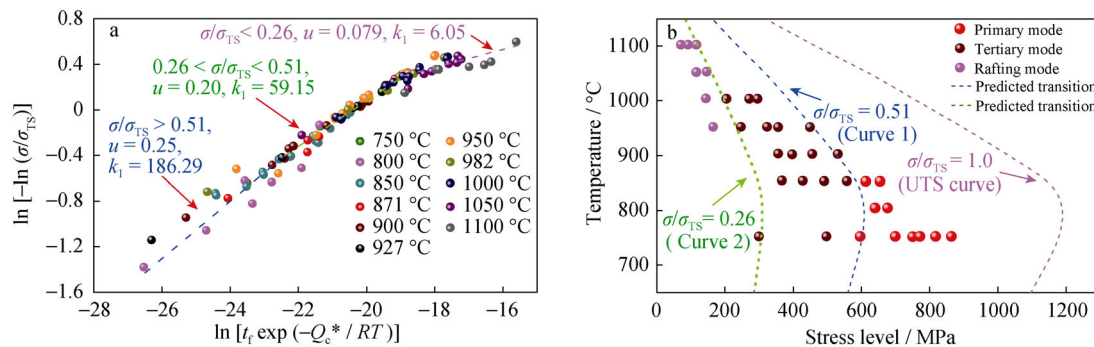


Fig. 7 Schematic expressed by $\ln[t_f \exp(-Q_c^*/RT)]$ versus $\ln[-\ln(\sigma/\sigma_{TS})]$ **a** and modes of creep deformation at different temperature–stress conditions **b** of CMSX-4 in [001] direction

activated processes are favored strongly. Fortunately, as shown in Fig. 7b, it is encouraging that different temperature–stress conditions required for the operation of these three modes in CMSX-4 are well simulated through the predicted break points (i.e., located at $\sigma/\sigma_{TS} = 0.26$ and 0.51) by Wilshire equations.

5.3 Further application of Wilshire equations

It is well known that the traditional Larson–Miller curve is widely used for appraising the stress rupture strength of different materials. This method is based on the concept of absolute stress to compare the creep properties. However, it is insufficient to only evaluate the creep properties of different materials from the perspective of absolute performance. Actually, in order to increase the safety factor and save costs, the engineers and designers are always looking forward to fully knowing the potential on creep properties of the adopted materials. It is easy to understand that when the same stress rupture life of two materials is satisfied simultaneously (at the same temperature), the material crept at a lower stress level normalized by UTS (σ/σ_{TS}) will be the safer choice. On the other hand, when the two materials are crept at the same σ/σ_{TS} (at the same temperature), the material with a longer rupture life will be the more economical choice for designers. Hence, in this section, it is tried to evaluate the creep properties of different materials from the perspective of relative performance to make full use of materials. Fortunately, it is obvious that one inherent property of the Wilshire equations is that the applied stress is normalized by UTS; especially, the superior prediction and extrapolation performance of this method are fully proved in a wide range of materials, and hence, a valuable alternative technique (named as Wilshire curve) to evaluate the creep properties in an innovative perspective is proposed here. For the first time, this new technique is conducted here for evaluating the stress rupture life of two typical DS Ni-based superalloys (i.e.,

DZ125 and DZ17G at L direction), and the Larson–Miller parametric method is conducted simultaneously for comparison. The Larson–Miller parameter is described as $P = T(20 + \lg t)/1000$, where T is the temperature in K and t is the stress rupture lifetime in h. The applied stress can be expressed using a polynomial of degree 3: $\lg \sigma = a_0 + a_1 P + a_2 P^2 + a_3 P^3$, where the parameters a_0, a_1, a_2, a_3 are fitted by testing data. As shown in Fig. 8a, the experimental data (i.e., applied stress vs. Larson–Miller parameter) of DZ125 and DZ17G are well fitted, which agrees with the conclusion that the Larson–Miller method gets good accuracy in predicting creep properties in a limit region of stress rupture life. The values of a_0 – a_3 of DZ125 are $-6.283, 1.108, -0.0408$ and 0.000434 , and they are $-11.83, 1.734, -0.0643$ and 0.000724 for DZ17G, respectively. As mentioned above, the parameters in Eq. (5) of Wilshire method can be fitted linearly by plotting $\ln[t_f \exp(-Q_c^*/RT)]$ against $\ln[-\ln(\sigma/\sigma_{TS})]$. For DZ125, the values of u and k_1 are 0.134 and 28.6 for $\sigma/\sigma_{TS} < 0.448$, while 0.203 and 178 for $\sigma/\sigma_{TS} > 0.448$. For DZ17G, the values of u and k_1 are 0.174 and 40.3 for $\sigma/\sigma_{TS} < 0.397$, while 0.239 and 165.8 for $\sigma/\sigma_{TS} > 0.397$. As shown in Fig. 8b, using the values of parameters, the stress rupture master curves can be plotted by Eq. (5) (x-axis is $t_f \exp(-Q_c^*/RT)$, and y-axis is the relative stress (σ/σ_{TS})), which exhibits good accuracy. However, our attention is not paid to the predicting ability of these two methods. We are encouraged to find that these two methods provide entirely different creep rupture performances. In Fig. 8a, the vertical axis is the absolute stress and DZ125 owns overall better creep rupture properties, but this superiority obviously decreases with the increase in P parameter. Conversely, when the vertical axis in Fig. 8b is the relative stress (i.e., UTS-normalized stress), the DZ17G owns entirely better creep rupture properties. That is to say, this simple but robust method developed by Wilshire and co-workers can be further used for evaluating creep properties (also including $\dot{\epsilon}_{min}$ and t_e) of different materials with an

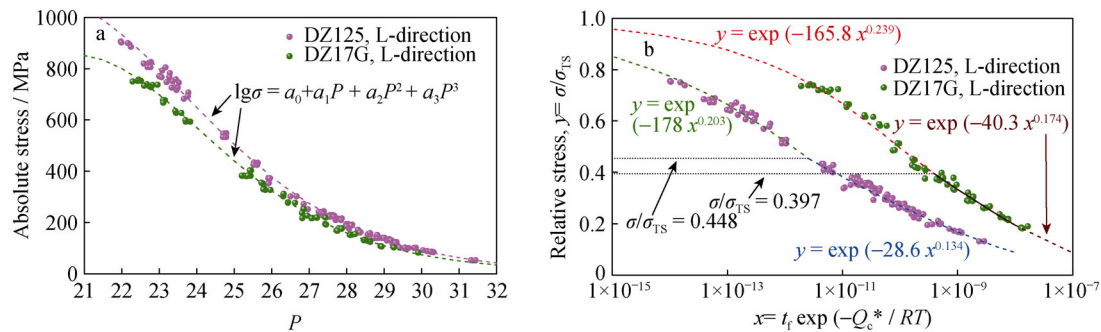


Fig. 8 Comparison of stress rupture properties of DZ125 and DZ17G by **a** Larson–Miller curve and **b** Wilshire curve

innovative perspective on making full use of creep properties.

6 Conclusion

In this paper, the capability of Wilshire equations in simulating typical creep characteristics in typical anisotropic Ni-based DS and SC superalloys was fully verified. Some principal conclusions are listed as follows. The obtained creep activation energy (Q_c^*) by Wilshire method is far closer to the activation energy for lattice diffusion of Ni-based superalloys than the value calculated traditionally. The flexibility of the orientation factor modified Wilshire equations is fully demonstrated by various data sets of DZ125 and DS GTD-111, where good simulations of the anisotropic t_f , $\dot{\epsilon}_{\min}$ and t_e are obtained.

The obtained ‘break point’ stress by Wilshire method is well consistent with the transition of creep deformation mechanism of CMSX-4 happened at different temperature–stress regions, which helps to provide physical confidence of this method. The Wilshire method is further used for evaluating typical creep properties of different materials with an innovative perspective on making full use of creep properties.

Acknowledgments This research was financially supported by the National Natural Science Foundation of China (No. 51275023) and the Innovation Foundation of BUAA for Ph.D. Graduates (No. YWF-14-YJSY-49).

References

- [1] Scholz A, Wang Y, Linn S. Modeling of mechanical properties of alloy CMSX-4. *Mater Sci Eng A*. 2009;510(10):278.
- [2] Liu H, Xuan FZ. A new model of creep rupture data extrapolation based on power processes. *Eng Fail Anal*. 2011;18(8):2324.
- [3] Harrison W, Whittaker M, Williams S. Recent advances in creep modelling of the nickel base superalloy, alloy 720Li. *Materials*. 2013;6(3):1118.
- [4] Lin YC, Xia YC, Chen MS. Modeling the creep behavior of 2024-T3 Al alloy. *Comput Mater Sci*. 2013;67:243.
- [5] Tamura M, Esaka H, Shinozuka K. Stress and temperature dependence of time to rupture of heat resisting steels. *ISIJ Int*. 1999;39(4):380.
- [6] Wilshire B, Scharming PJ. A new methodology for analysis of creep and creep fracture data for 9 %–12 % chromium steels. *Int Mater Rev*. 2008;53(2):91.
- [7] Wilshire B, Scharming PJ, Hurst R. New methodology for long term creep data generation for power plant components. *Mater Sci Eng Syst*. 2007;2(2):84.
- [8] Li SX, Ellison EG. The influence of orientation on the elastic and low cycle fatigue properties of several single crystal nickel base superalloys. *J Strain Anal Eng Des*. 1994;29(2):147.
- [9] Han GM, Yu JJ, Sun YL. Anisotropic stress rupture properties of the nickel-base single crystal superalloy SRR99. *Mater Sci Eng A*. 2010;527(21):5383.
- [10] Yuan C, Guo JT, Yang HC. Deformation mechanism for high temperature creep of a directionally solidified nickel-base superalloy. *Scripta Mater*. 1998;39(7):991.
- [11] China Aeronautical Materials Handbook Editorial Board. *China Aeronautical Materials Handbook*, vol. 2. 2nd ed. Beijing: Standards Press of China; 2002. 113.
- [12] Meng XL. *Microstructure and creep behaviours of DZ125 nickel based superalloy*. Shenyang: Shenyang University of Technology; 2012. 145.
- [13] Yuan C, Guo JT, Yang HC. Effect of grain boundary orientation and cyclic load on creep and fracture behaviour in directionally solidified nickel base superalloy. *Mater Sci Tech Lond*. 2002;18(1):73.
- [14] Ibanez AR, Srinivasan VS, Saxena A. Creep deformation and rupture behaviour of directionally solidified GTD 111 superalloy. *Fatigue Fract Eng Mater*. 2006;29(12):1010.
- [15] Gordon AP. *Crack Initiation modeling of a directionally-solidified nickel-base superalloy*. Atlanta: Georgia Institute of Technology; 2006. 123.
- [16] Ibanez AR. *Modeling creep behavior in a directionally solidified nickel base superalloy*. Atlanta: Georgia Institute of Technology; 2003. 75.
- [17] MacLachlan DW, Knowles DM. Modeling and prediction of the stress rupture behaviour of single crystal superalloys. *Mater Sci Eng A*. 2001;302(2):275.
- [18] Ma A, Dye D, Reed RC. A model for the creep deformation behaviour of single-crystal superalloy CMSX-4. *Acta Mater*. 2008;56(8):1657.
- [19] Woodford DA. Parametric analysis of monocrystalline CMSX-4 creep and rupture data. *Metall Mater Trans A*. 1998;29(10):2645.
- [20] Monkman FC, Grant NJ. An empirical relationship between rupture life and minimum creep rate in creep-rupture tests. *Proc ASTM*. 1956;56:593.

- [21] Mukherjee AK, Bird JE, Dorn JE. Experimental correlations for high-temperature creep. *Trans ASM*. 1969;62:155.
- [22] Evans M. Prediction of long-term creep rupture data for 18Cr–12Ni–Mo steel. *Int J Press Vessels Pip*. 2011;88(11):449.
- [23] Liu JL, Jin T, Sun XF. Anisotropy of stress rupture properties of a Ni base single crystal superalloy at two temperatures. *Mater Sci Eng A*. 2008;479(1):277.
- [24] Whittaker MT, Harrison WJ, Lancaster RJ. An analysis of modern creep lifing methodologies in the titanium alloy Ti6-4. *Mater Sci Eng A*. 2013;577(15):114.
- [25] Sajjadi SA, Nategh S. A high temperature deformation mechanism map for the high performance Ni-base superalloy GTD-111. *Mater Sci Eng A*. 2001;307(1):158.
- [26] Reed RC. *The Superalloys: Fundamentals and Applications*. Cambridge: Cambridge University Press; 2006. 154.